

UKAEA-CCFE-PR(25)400

M B Dreval, K G McClements, R Ochoukov, H J C  
Oliver, D Ryan, R Sarwar, R Scannell, S E Sharapov,  
A Stephen, R. Dendy, MAST Upgrade Team

# **First observations of two-type energetic particle-driven ion cyclotron emission in MAST-U**

Enquiries about copyright and reproduction should in the first instance be addressed to the UKAEA Publications Officer, Culham Science Centre, Building K1/O/83 Abingdon, Oxfordshire, OX14 3DB, UK. The United Kingdom Atomic Energy Authority is the copyright holder.

The contents of this document and all other UKAEA Preprints, Reports and Conference Papers are available to view online free at [scientific-publications.ukaea.uk/](https://scientific-publications.ukaea.uk/)

# **First observations of two-type energetic particle-driven ion cyclotron emission in MAST-U**

M B Dreval, K G McClements, R Ochoukov, H J C Oliver, D Ryan,  
R Sarwar, R Scannell, S E Sharapov, A Stephen, R. Dendy, MAST  
Upgrade Team



# First observations of two-type energetic particle-driven ion cyclotron emission in MAST-U

M B Dreval<sup>1</sup>, K G McClements<sup>2</sup>, R Ochoukov<sup>3</sup>, H J C Oliver<sup>2</sup>, D Ryan<sup>2</sup>, R Sarwar<sup>2</sup>, R Scannell<sup>2</sup>, S E Sharapov<sup>2</sup>, A Stephen<sup>2</sup>, R. Dendy<sup>4</sup>, MAST Upgrade Team<sup>a</sup>

<sup>1</sup>Institute of Plasma Physics, National Science Center, Kharkov Institute of Physics and Technology, 61108 Kharkov, Ukraine

<sup>2</sup>UKAEA, Culham Campus, Abingdon OX14 3DB, UK

<sup>3</sup>Max-Planck-Institute for Plasma Physics, Boltzmannstrasse 2, 85748 Garching, Germany

<sup>4</sup>Centre for Fusion, Space and Astrophysics, University of Warwick, Coventry, United Kingdom of Great Britain and Northern Ireland

<sup>a</sup>See Harrison et al 2019 Nucl. Fusion 59 11201.

## Abstract

The first measurements of energetic particle-driven ion cyclotron emission (ICE) in the Mega-Amp Spherical Tokamak Upgrade (MAST-U) have been obtained by adding a high sampling rate (250MHz) capability to one coil of the existing OMAHA array, oriented to measure fluctuations in the toroidal magnetic field component. All these measurements were carried out in pulses with either on-axis neutral beam injection (NBI) only, or a combination of on-axis and off-axis NBI. Two types of energetic particle-driven ICE have been detected: a narrow band emission with some frequency splitting at harmonics of the on-axis deuterium cyclotron frequency,  $f_c^D$ , and a broader-band emission harmonically-structured with peak frequencies corresponding to the harmonics of  $f_c^D$  at the outboard (low field side) plasma edge.

## 1. Introduction

Diagnosis of fast ion populations will be crucial in magnetic fusion machines, and specifically – in future DT fusion reactors based on plasma heating by alpha-particles. One promising method of the fast ions distribution diagnosis is an analysis of ion cyclotron emission (ICE)—a collective process in which spectral peaks are generated at harmonics of the ion cyclotron frequency ( $f_{ci}$ ). The ICE excited by energetic ions such as fusion products or beam-injected ions could potentially deliver important information on the types of ions, their distribution function in velocity space, and spatial localization. The relationship between ICE spectra and the underlying fast ion distribution remains insufficiently understood, however, thus highlighting the need for an improved theory/modelling, together with dedicated ICE diagnostics and targeted experimental studies. Sometimes ICE is observed at the outer edge of the plasma in tokamaks such as JET [1, 2], TFTR [3, 4], JT-60U [5], ASDEX Upgrade [6], DIII-D [7], KSTAR [8, 9], EAST [10] and stellarators such as LHD [11] and W7-X[12]. This type of ICE is characterized by broader-band but still harmonically-structured emission with peak frequencies corresponding to harmonics of  $f_c^D$  closer to the outboard plasma edge, and with the dominant polarization of the wave corresponding to compressional Alfvén perturbations. This type of emission can be considered as a broadband continuum-like emission without discrete eigenmodes. ICE from the plasma core has been also described more recently on DIII-D [13-15], ASDEX Upgrade [6, 16–19], EAST [20], TUMAN-3M [21], and JT-60U [22,23] and TCV [24]. In the spherical tokamaks NSTX and NSTX-U, where the plasma conditions are closest to those in MAST-U, ICE has been observed at mid-radius [25], exhibiting a strongly chirping character [26]. The core ICE is of narrower-band in frequency and it differs from the broadband edge ICE in several aspects: a) the very close proximity of the mode frequencies to the on-axis ion cyclotron harmonics,

b) fine splitting of the modes, c) the excellent tracking of the magnetic field variation by the mode frequency. These narrower-band ICE perturbations evidently indicate they originate from corresponding eigenmodes like, e.g., described in [27].

Most of the theories and modeling developed for ICE interpretation so far were using the assumption that the ICE were compressional Alfvén eigenmodes (CAEs). However, dedicated CAE experiments on MAST [28] exhibited a fairly broad-band CAE spectrum, but without any clearly peaked amplitudes near the ion cyclotron harmonics. Further studies of the discrete core ICE developed recently an alternative theory [27] to be further validated in future experiments.

One of the most robust and reliable diagnostic methods for detecting electromagnetic waves in plasmas is the use of a B-dot probe, also known as a Mirnov coil or magnetic probe [29]. These probes are widely employed to study various MHD modes in the low-frequency range. Dedicated B-dot probes could be also employed for detecting high-frequency modes, such as ion cyclotron emission (ICE) modes. To detect MHD modes, a set of OMAHA coils with a digitization rate of 10 MHz was used on MAST and MAST-U, enabling measurements up to 5 MHz [30]. These coils were previously used in MAST for the characterization of compressional Alfvén eigenmodes (CAE) [31]. In the MAST-U tokamak, no energetic particle-driven emission has been detected so far at the deuterium ion cyclotron frequency. This is consistent with the absence of instabilities observed previously using OMAHA coils in the 1.0–2.5 MHz range, where global Alfvén eigenmodes are often detected [25,26,31], and is also consistent with the system’s upper measurement limit of 5 MHz. Although the bandwidth of the OMAHA coils is expected to be substantially higher than the 5 MHz limitation imposed by the old data acquisition system, as suggested by Fig. 7 in Ref. [30], the data acquisition frequency range limitation has constrained prior measurements. In our work, the first test measurements of energetic particle-driven ion cyclotron emission (ICE) in MAST-U have been obtained by adding a high sampling rate (250 MHz) capability to one coil of the existing OMAHA array. One OMAHA coil, oriented to measure fluctuations in the toroidal magnetic field component, was directly connected to the new ADC—bypassing the low-pass filter, preamplifier, and matching circuit of the original system.

## 2. Experimental conditions and ICE modes observation in MAST-U

MAST Upgrade [32] (MAST-U) retains the same aspect ratio ( $R/a = 0.85/0.65 \approx 1.3$ ) of MAST [33], but has new capabilities, including a set of new poloidal field coils for highly flexible plasma shaping, a higher toroidal field and plasma current. Looking down from above MAST-U, as well as MAST, the equilibrium toroidal field is in the clockwise direction, while the inductive plasma current and NBI are in the anti-clockwise direction. MAST-U is equipped with two NBI injection systems. One of the MAST-U NBI “SS” systems deposits fast ions on-axis and the second “SW” system deposits fast ions off-axis, ~65 cm above the equatorial plane [32]. This geometry allows us to tailor the fast particle deposition profile to design studies of fast ions [34] and AEs excited by these fast ions. The ICE modes under consideration are observed in MAST-U discharges with on-axis NBI injection and combined on-axis and off-axis NBI discharges. These modes have been observed in low density, high electron and ion temperature, and high fusion neutron rate discharges, in contrast to the higher density discharges where the numerous GAEs were analyzed [31]. An overview of 0.75 MA MAST-U discharge where ICE modes were observed is shown in Figure 1.

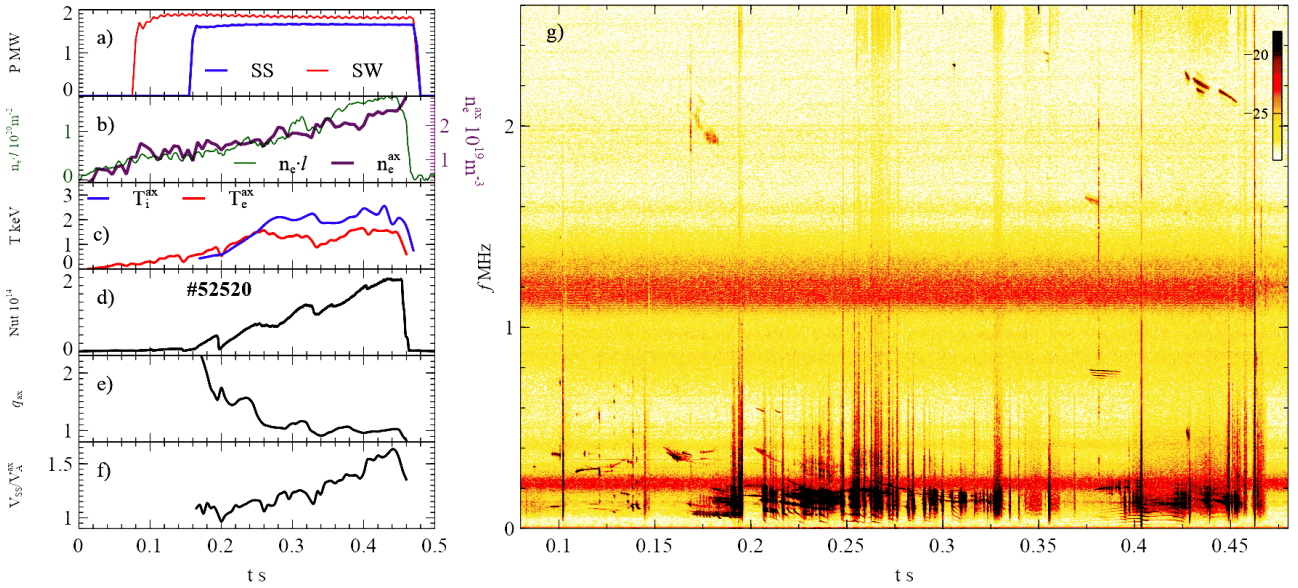


Fig.1 Time traces of a) on-axis “SS” and of-axis “SW” NBI power, b) line-integrated density and density at magnetic axis, c) electron and ion temperatures at the magnetic axis, d) temporal evolution of fusion neutron rate, e) safety factor evolution at the magnetic axis, f) ratio between the “SS” beam velocity and Alfvén velocity at the magnetic axis , g) magnetic spectrogram of conventional OMAHA system in MAST-U discharge #52520,  $B_T=0.55T$ ,  $I_p=0.75MA$ .

An overview of 1 MA MAST-U discharge where ICE modes were observed is shown in Figure 2. The not-monotonic temporal evolution of such discharge parameters, such as the as neutron rate, indicates that MHD instabilities such as the internal reconnection events prevent further improvements of the plasma parameters.

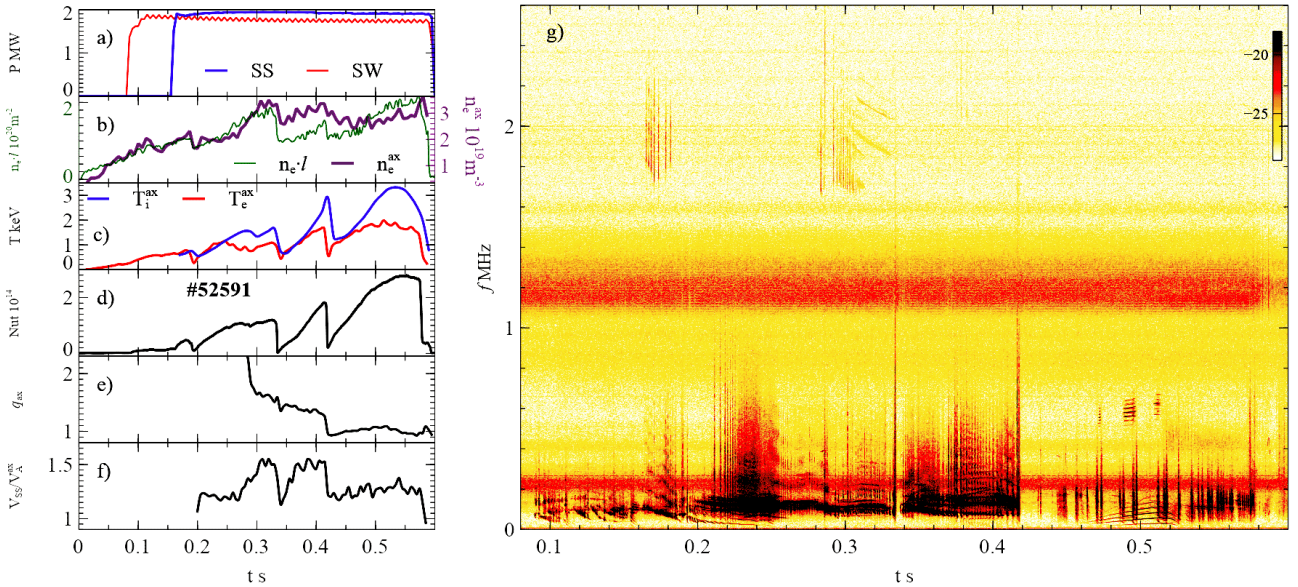


Fig.2 Time traces of a) on-axis “SS” and of-axis “SW” NBI power, b) line-integrated density and density at the magnetic axis, c) electron and ion temperatures at the magnetic axis, d) temporal evolution of the fusion neutron rate, e) temporal evolution of the safety factor at the magnetic axis, f) ratio between the “SS” beam velocity and Alfvén velocity at the magnetic axis , g) magnetic spectrogram of the conventional OMAHA system in MAST-U discharge #52591,  $B_T=0.67T$ ,  $I_p=1MA$ , for which equilibrium with MSE correction was reconstructed.

The radial profiles of the key plasma parameters in the 0.75 MA and 1 MA discharges of MAST-U are shown in Fig.3. One can see that the density profile has rather significant “ears” (increases) at

the plasma edge, and both electron and ion temperatures are pretty high,  $\sim 1.5$  keV and  $\sim 3$  keV correspondingly.

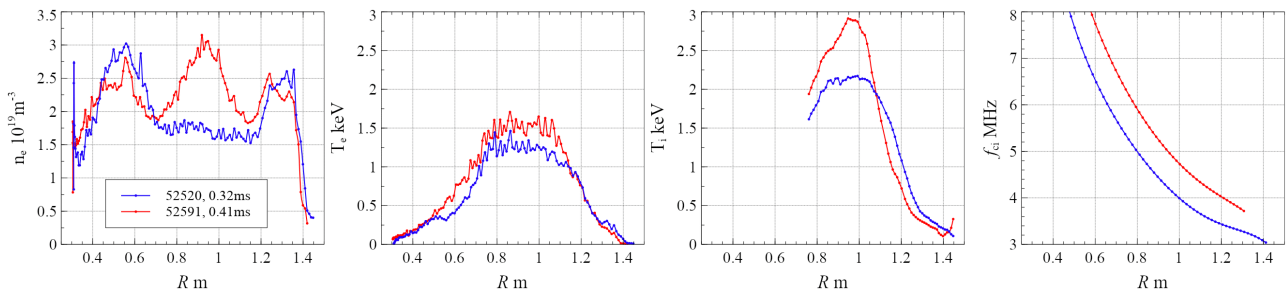


Fig.3 (from left to right): Radial profiles of the electron density and temperature measured by Thomson scattering; Ion temperature profiles measured via  $C^{5+}$  impurity; The ion cyclotron frequency profiles at 0.32 s in MAST-U discharge #52520 (in blue) and at 0.41 s in #52591 (in red).

Various energetic particle-driven modes including modes in CAE/GAE frequency range are seen in low density MAST-U discharges #52520 and #52591 by the conventional OMAHA system. In such low or moderate density discharges, modes in the ICE frequency range is also seen, as Figure 4 shows.

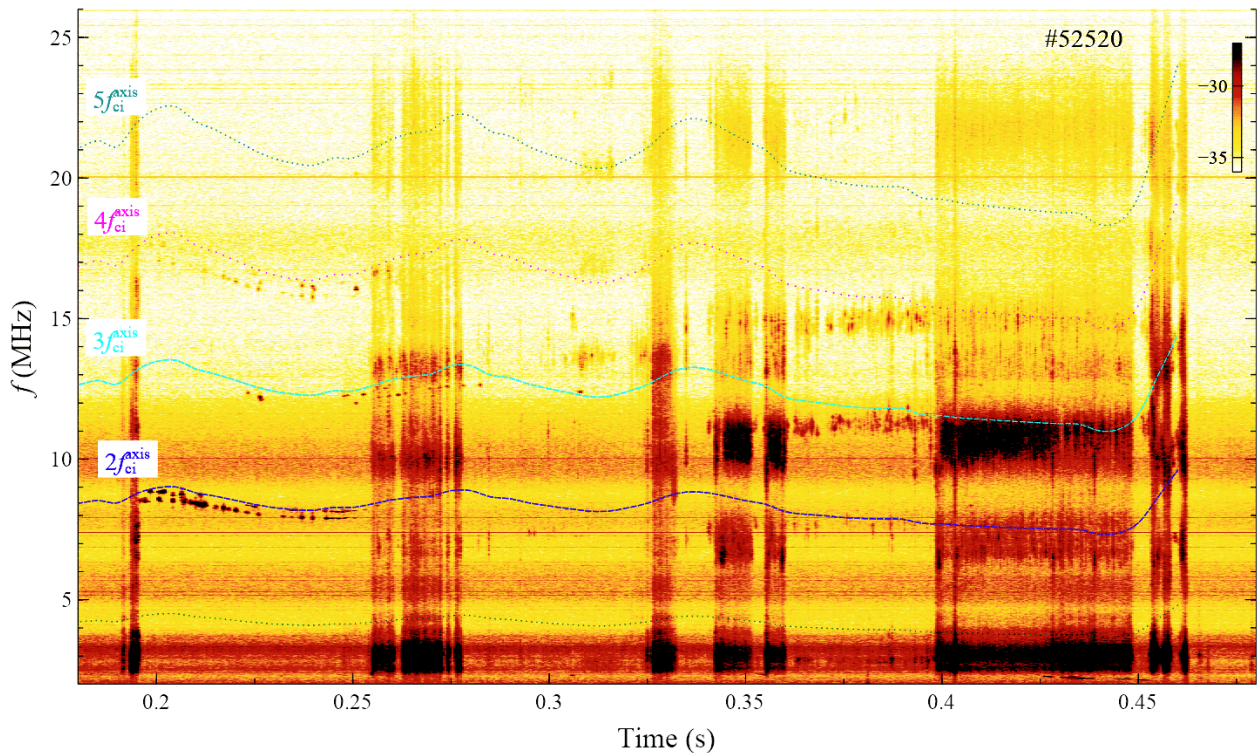


Fig.4 Magnetic spectrogram of the high-frequency test OMAHA system and the cyclotron harmonics of deuterium ions at the magnetic axis in MAST-U discharge #52520.

Two distinctively different types of ICE perturbations in the frequency range of ion cyclotron harmonics are observed almost simultaneously in MAST-U discharge #52420: one of them is a broadband in frequency, while the other one is a narrowband. The frequency of the narrowband modes appears slightly below (2-8%) the cyclotron harmonics of the deuterium ions at the magnetic axis. A frequency shift of a few percent from the cyclotron harmonics at the magnetic axis indicates that these modes are core ICE. The frequencies of these modes follow the harmonics of the cyclotron frequency at the magnetic axis, as seen in the figure. Core ICE modes at the 2<sup>nd</sup>, 3<sup>rd</sup>, and 4<sup>th</sup> harmonics are observed between 0.2 and 0.3 s in Fig. 4. These modes are not observed at the 1<sup>st</sup> ion cyclotron harmonic or below, and therefore cannot be detected by the conventional OMAHA system. The second type of ICE is the broadband emission, observed near 0.2, 0.25, 0.35, and 0.4–0.45 s. The

low-frequency part of this ICE is slightly visible with the conventional OMAHA system in the 2.6–2.8 MHz range (see Fig.1). This broadband ICE still exhibits a harmonically-structured frequency emission, with the peak frequencies corresponding to harmonics of the deuterium cyclotron frequency  $f_{cD}$ , but at the outboard plasma edge. Broadband modes below the 1<sup>st</sup>–6<sup>th</sup> harmonics, with a maximum amplitude below the 3<sup>rd</sup> and 1<sup>st</sup> harmonics, are seen in Fig.4. In spite of 250 MHz sampling rate of the new OMAHA system, the bandwidth of the OMAHA coil itself can be limited [30]. Thus, we cannot conclude that the modes above the 6<sup>th</sup> harmonics are absent. The frequencies of this ICE emission bands do not follow the time variation of the cyclotron harmonics.

## 2. Experimental properties of broadband ICE

The frequency of the broadband modes is not only weakly sensitive to the cyclotron frequency, but it also shows a rather weak dependence on other plasma parameters, such as density, temperature, and equilibrium, as seen in Figs. 1 and 4. This weak sensitivity suggests that the broadband modes are not associated with discrete eigenmodes, but may instead be formed by continuum modes. The appearance of these broadband modes is determined primarily by the ratio of drive to damping, as no well-defined eigenfunctions are involved. Very low plasma density appears to be a key condition for the observation of this type of mode. So far, these modes have been observed only in combined NBI discharges with both on-axis and off-axis injection. However, this is a preliminary conclusion due to the rather limited number of MAST-U discharges with the high-frequency OMAHA diagnostics. It looks likely that the excitation of these modes may strongly depend on the discharge conditions, in contrast to their frequency, which remains almost constant. Indirect evidence of an interplay between energetic particle redistribution, low-frequency modes, and a broadband ICE excitation is seen in the simultaneous behavior of low-frequency modes and ICE. In particular, a rapid transition from LLM modes to fishbone-like modes accompanied with excitation of the broadband ICE modes are observed, as shown in Fig. 5.

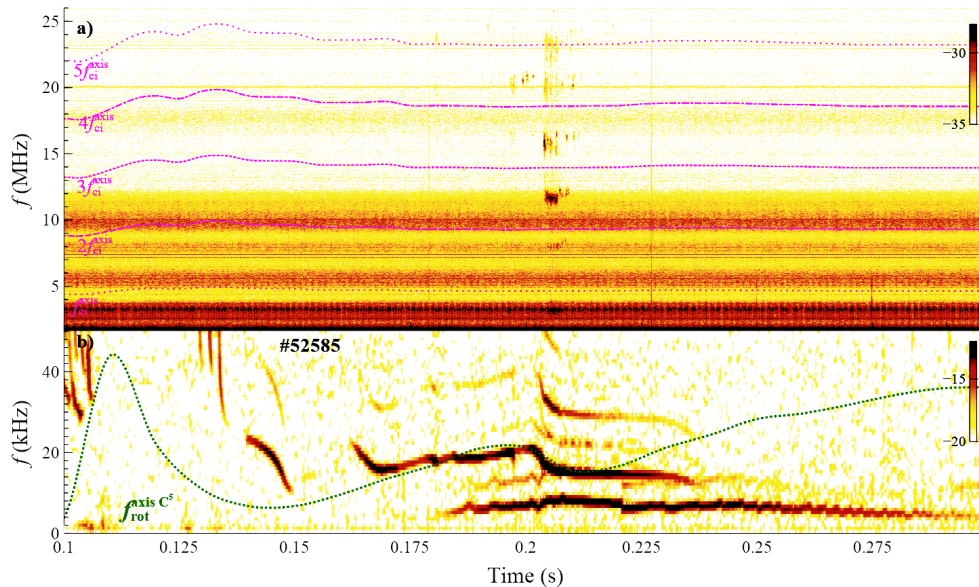


Fig.5 Magnetic spectrogram of a) new OMAHA system and cyclotron harmonics of deuterium ion at magnetic axis, b) conventional OMAHA system and toroidal plasma rotation measured by carbon impurity at magnetic axis in MAST-U discharge #52585 with SS and SW NBI.

In discharge #52585, the distribution of broadband ICE amplitudes around the cyclotron harmonics differs from that observed in discharge #52520. This observation highlights the complex nature of the broadband ICE drive and damping mechanisms. The appearance of 20 MHz modes prior to both the fishbone activity and the emergence of other ICE harmonics in discharge #52585 further emphasizes this complexity.

### 3. Experimental properties of core ICE

The core ICE modes are not observed at the 1<sup>st</sup> ion cyclotron harmonic or below, and therefore cannot be detected by the conventional OMAHA system. A similar absence of ICE emission near the 1<sup>st</sup> ion cyclotron harmonic in deuterium plasmas with deuterium NBI has been reported in other tokamaks, such as ASDEX-U [16]. This appears to be one of the fundamental properties of core ICE emission. Core ICE near 2<sup>nd</sup> -6<sup>th</sup> deuterium ion cyclotron harmonics is observed in Fig.6.

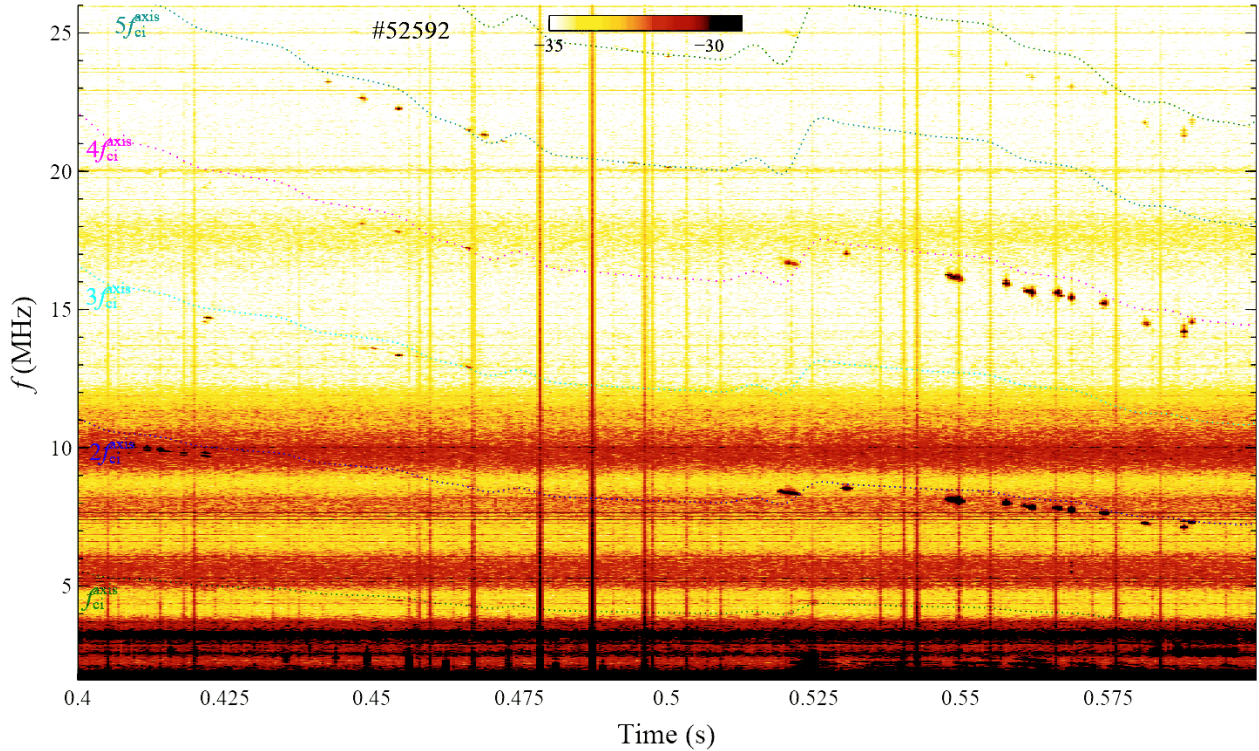


Fig.6 Magnetic spectrogram of new OMAHA system and cyclotron harmonics of deuterium ions at the magnetic axis in MAST-U discharge #52592 with SS and SW NBI.

We cannot analyze frequencies above 25 MHz due to the bandwidth limitations of the OMAHA coil, as is also the case for the broadband modes. The appearance of different core ICE harmonics appears to be largely independent from one another, as seen in Figs. 4 and 6. This observation underscores the complex nature of the core ICE drive and damping mechanisms similar to what is observed for the broadband ICE. Another notable feature of the core ICE in MAST-U is the absence of long-lasting continuous ICE modes. In all observed MAST-U cases, core ICE consists of a series of short bursts. These bursts are likely to be synchronized with certain core plasma events, consistent with their localization in the plasma core. The interaction between ICE and sawtooth activity was observed in JET [37]. An interplay between bursty MHD events and ICE was recently reported in LHD [38]. An example of a single on-axis NBI discharge exhibiting core ICE bursts is shown in Fig. 7.

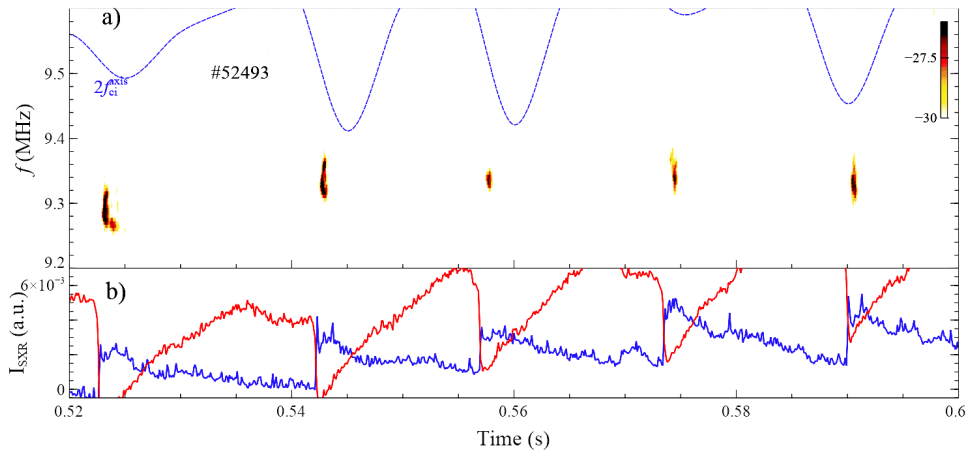


Fig.7 a) Magnetic spectrogram of new OMAHA system and 2<sup>nd</sup> cyclotron harmonic of deuterium ions at the magnetic axis and b) an inversion of the amplitude of Soft X-ray emission seen from core (red) and edge (blue) SXR channels in MAST-U discharge #52493 with SS NBI only.

These bursts are synchronized with the Sawtooth inversions' times, as evidenced by the inversion of the soft X-ray (SXR) emission shown in the figure. This provides an additional experimental evidence supporting the core localization of the narrowband ICE modes, since the inversion region is confined in the plasma core near the  $q=1$  flux surface. The sawtooth inversions strongly affect the core region inside the  $q=1$  surface, while having a much weaker impact on the larger volume outer plasma. Therefore, the observed correlation between core ICE and the Sawtooth instability cycle indicates that the core ICE emission originates from a region near or inside the  $q=1$  surface. The interplay between the sawtooth inversion and ICE can be associated with modifications of the plasma equilibrium, and in particular, with strong changes in the safety factor ( $q$ ) profile. According to Ref. [27], the ICE eigenmodes are sensitive to the  $q$ -profile. Another factor involved in this interaction is the strong modification of the fast-ion distribution by sawteeth, which in turn affects the ICE drive and/or damping. The problem of fast-ion redistribution by sawteeth and its interplay with the EAE mode was recently investigated in JET [39]. In that study, the redistribution was found to excite EAEs near the  $q = 1$  surface, according to the experimental measurements reported. We expect a similar impact of sawteeth on the core plasma region, and a weaker influence in the outer region, in the case of ICE modes in MAST-U as well. A zoomed view of the sawtooth inversion and ICE emission near the second harmonic is shown in Fig. 8.

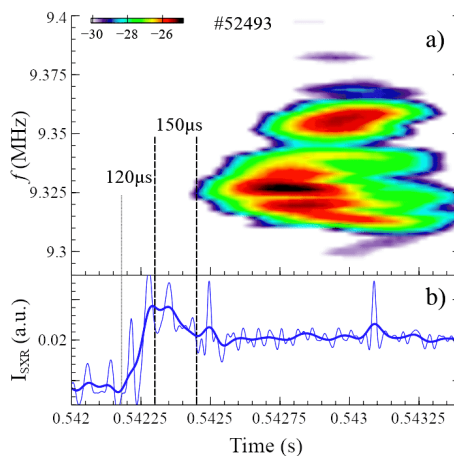


Fig.8 Zoomed figure 7. a) Magnetic spectrogram of new OMAHA system b) edge SXR signal, showing the rise in emission at a sawtooth crash. The bold curve is a running average of the faint curve. Times between the sawtooth inversion start, inversion end and ICE mode start are marked by dashed lines. The time delays between these events are depicted in the picture. MAST-U discharge #52493 with SS NBI only.

The ICE emission appears after the end of the inversion phase, with a short delay of about 150  $\mu$ s. Occasionally, the core ICE bursts can last longer, as Figure 9 shows.

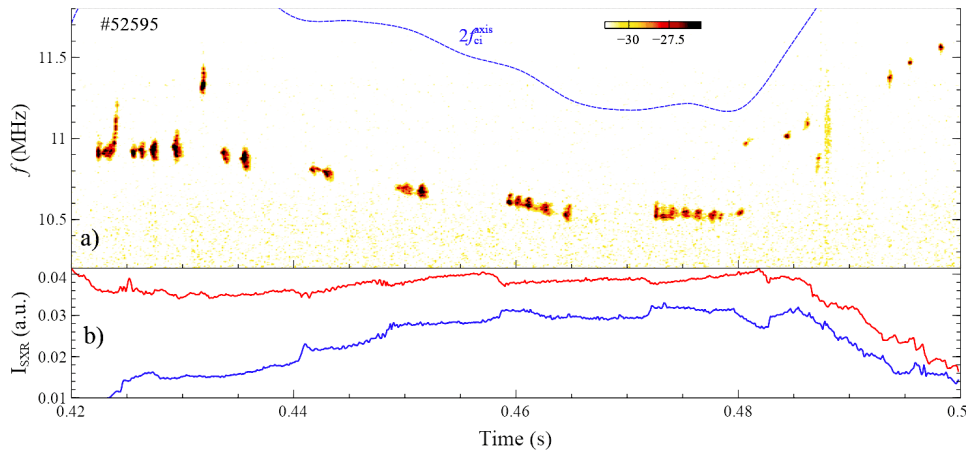


Fig.9 a) Magnetic spectrogram of new OMAHA system and the 2<sup>nd</sup> cyclotron harmonic of deuterium ions at the magnetic axis and b) an inversion of the amplitude of Soft X-ray emission seen from core (red) and edge (blue) SXR channels in MAST-U discharge #52495 with SS and SW NBI.

Some weaker inversions are also visible in Fig. 9. The core ICE emission is observed during certain periods following these inversions, although it still does not appear as continuous lines. This observation suggests that ICE emission is influenced by additional factors beyond the sawtooth inversions alone and/or some nonlinear effects.

Another characteristic feature of the core ICE is the fine splitting of the frequency into a set of closely spaced narrowband branches, a phenomenon observed in various tokamaks [14–16]. The doublet splitting of the cyclotron harmonics and the resulting need to invoke nonlinear interactions with lower harmonics of substantial amplitude were reported recently [35,36]. Another approach, based on the coexistence of a set of eigenmodes considered in Ref. [27], can also explain multiple splitting. This splitting is visible in Fig. 4. Two distinct sets of modes can also be seen at 0.43 s and 0.48 s in Fig. 9. An example of even more complex fine splitting in core ICE modes is shown in Fig. 10.

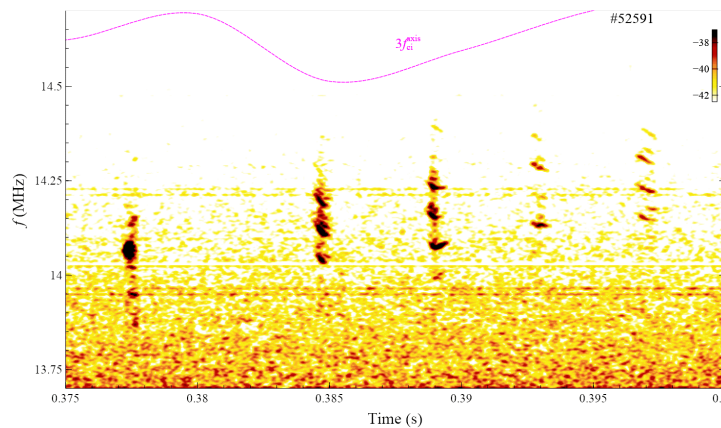


Fig.10 Magnetic spectrogram of new OMAHA system and the 3<sup>rd</sup> cyclotron harmonic of deuterium ions at the magnetic axis in MAST-U discharge #52591 with SS and SW NBI.

Features of the core ICE such as its narrowband nature, fine spectral splitting, and alignment with cyclotron harmonics indicate that this type of emission is determined by discrete eigenmodes—unlike the broadband ICE case. Therefore, the ICE modes exist due to the thermal plasma, while excitation

of core ICE modes by energetic ions depends on the competition between the drive due to the fast ions and damping due to the thermal plasma.

#### 4. Summary and conclusions.

The first measurements of energetic particle-driven ion cyclotron emission (ICE) in the Mega-Amp Spherical Tokamak Upgrade (MAST-U) have been obtained by adding a high-sampling-rate (250 MHz) capability to one coil of the existing OMAHA array, which is oriented to measure fluctuations in the toroidal component of the magnetic field. All measurements were carried out in pulses using either pure on-axis neutral beam injection (NBI) or a combination of on-axis and off-axis NBI.

Two types of energetic particle-driven ICE have been detected so far:

1. **Narrow-band emission**, with some evidence of frequency splitting, at harmonics of the on-axis deuterium cyclotron frequency,  $f_{cD}$ .
2. **Broadband but still harmonically-structured emission**, with peak frequencies corresponding to harmonics of  $f_{cD}$  near the outboard plasma edge.

The following features of the **core ICE** have been observed:

- a) Very close alignment of mode frequencies with ion cyclotron harmonics
- b) Fine splitting of the modes
- c) Excellent tracking of magnetic field variations by the mode frequencies

The core ICE appears to correspond to discrete eigenmodes. In all observed MAST-U cases, core ICE consists of a series of short bursts. These bursts are synchronized with certain core plasma events—such as sawtooth inversions—consistent with localization in the plasma core. No core ICE has been detected at the fundamental deuterium ion cyclotron frequency itself. This is consistent with the absence of detected instabilities using OMAHA in the range 1.0–2.5 MHz (where global Alfvén eigenmodes are often observed), and with the upper measurement limit of these coils, which is typically 5 MHz.

The following features of the **broadband ICE** have been observed:

- a) Broad peaks near harmonics of the edge cyclotron frequency
- b) Weak sensitivity of the frequency spectra to variations in plasma parameters, including the on-axis cyclotron frequency

Broadband ICE appears to be associated with continuum modes. Its appearance is linked to specific discharge conditions. In one pulse, ICE was detected only during a large-amplitude fishbone event, suggesting that the emission was triggered by energetic ion redistribution.

Both core ICE and broadband ICE have been observed in low-density discharges.

So far, measurements have only been taken at a single toroidal location. As a result, no information is currently available regarding toroidal mode numbers. However, there are plans to upgrade the system in the next MAST-U campaign—scheduled to begin in November 2025—to enable such measurements.

#### Data availability statement

The data generated and/or analysed during the current study are not publicly available for legal/ethical reasons but are available from the corresponding author on reasonable request.

#### Acknowledgments

This work has been carried out within the framework of the EUROfusion Consortium, funded by the European Union via the Euratom Research and Training Programme (Grant Agreement No. 101052200—EUROfusion). Views and opinions expressed are however those of the author(s) only and do not necessarily reflect those of the European Union or the European Commission. Neither the European Union nor the European Commission can be held responsible for them. The work has also been supported by the EPSRC Energy Programme (grant number EP/W006839/1), by the Simon Foundation and by the National Research Foundation of Ukraine (grant 2023.03/0101).

## ORCID iDs

M. Dreval <https://orcid.org/0000-0003-0482-0981>  
K G McClements <https://orcid.org/0000-0002-5162-509X>  
R. Ochoukov <https://orcid.org/0000-0002-5936-113X>  
S.E. Sharapov <https://orcid.org/0000-0001-7006-4876>

## Reference

- [1] Cottrell G.A. and Dendy R.O. 1988 *Phys. Rev. Lett.* **60** 33
- [2] Cottrell G.A. et al 1993 *Nucl. Fusion* **33** 1365
- [3] Cauffman S., Majeski R., McClements K.G. and Dendy R.O. 1995 *Nucl. Fusion* **35** 1597
- [4] Dendy R.O., McClements K.G., Lashmore-Davies C.N., Cottrell G.A., Majeski R. And Cauffman S. 1995 *Nucl. Fusion* **35** 1733
- [5] Ichimura M., Higaki H., Kakimoto S., Yamaguchi Y., Nemoto K., Katano M., Ishikawa M., Moriyama S. And Suzuki T. 2008 *Nucl. Fusion* **48** 035012
- [6] Ochoukov R. et al 2018 *Rev. Sci. Instrum.* **89** 10J101
- [7] Thome K.E., Pace D.C., Pinsker R.I., Meneghini O., del Castillo C.A. and Zhu Y. 2018 *Rev. Sci. Instrum.* **89** 10I102
- [8] Chapman B., Dendy R.O., McClements K.G., Chapman S.C., Yun G.S., Thatipamula S.G. and Kim M.H. 2017 *Nucl. Fusion* **57** 124004
- [9] Chapman B., Dendy R.O., Chapman S.C., McClements K.G., Yun G.S., Thatipamula S.G. and Kim M.H. 2018 *Nucl. Fusion* **58** 096027
- [10] Liu L.N. et al 2019 *Rev. Sci. Instrum.* **90** 063504
- [11] Reman B.C.G., Dendy R.O., Akiyama T., Chapman S.C., Cook J.W.S., Igami H., Inagaki S., Saito K. and Yun G.S. 2019 *Nucl. Fusion* **59** 096013
- [12] D. Moseev, R. Ochoukov, M. Dreval, I. Kuzmych, P. Aleynikov, K. Aleynikova, S. Bozhenkov, R.Dendy, D. Hartmann, J.-P. Kallmeyer, Ye. O. Kazakov, L. Krier, H.P. Laqua, S. Marsen, K.McClements, J. Ongena, J.W. Oosterbeek, S. Ponomarenko, B. Reman, J. Riemann, M. Salewski, O. Samant, D. Straus, B.S. Schmidt, T. Schröder, B. Schweer, T. Stange, R.C. Wolf, J. Zimmermann Ion cyclotron emission from ECRH-heated plasmas in Wendelstein 7-X submitted to *Physics of Plasmas* 2025
- [13] Thome K.E., Pace D.C., Pinsker R.I., Van Zeeland M.A., Heidbrink W.W. and Austin M.E. 2019 *Nucl. Fusion* **59** 086011
- [14] DeGrandchamp G. H. , Lestz J. B. , Van Zeeland M. A., Du X. D. , Thome K. E., Crocker N. A. , Heidbrink W. W. , and Pinsker R. I. , 2022 *Nucl. Fusion* **62** 106033
- [15] DeGrandchamp G. H., Heidbrink W. W., Du X. D. , Lestz J. B., Kim E.-H., Van Zeeland M. A., Boedo J. A., Thome K. E. , Crocker N. A. , Pinsker R. I. 2025 *Phys. Plasmas* **32** 032508
- [16] Ochoukov R. et al 2019 *Nucl. Fusion* **59** 014001
- [17] Chapman B., Dendy R.O., Chapman S.C., Holland L.A., Irvine S.W.A. and Reman B.C.G. 2020 *Plasma Phys. Control. Fusion* **62** 055003
- [18] Chapman B., Dendy R.O., Chapman S.C., McClements K.G. and Ochoukov R. 2020 *Plasma Phys. Control. Fusion* **62** 095022

- [19] Lunan Liu et al 2021 *Nucl. Fusion* **61** 026004
- [20] Liu L. et al 2020 *Nucl. Fusion* **60** 044002
- [21] Askinazi L.G., Belokurov A.A., Gin D.B., Kornev V.A., Lebedev S.V., Shevelev A.E., Tukachinsky A.S. and Zhubr N.A. 2018 *Nucl. Fusion* **58** 082003
- [22] Kimura H. et al 1998 *Nucl. Fusion* **38** 1303
- [23] Sumida S., Shinohara K., Ikezoe R., Ichimura M., Sakamoto M., Hirata M. and Ide S. 2019 *Plasma Phys. Control. Fusion* **61** 025014
- [24] A. J. van Vuuren, Nuclear Fusion to be submitted (2025).
- [25] Fredrickson E.D., Gorelenkov N., Bell R., Diallo A., LeBlanc B. and Podestà M. 2019 *Phys. Plasmas* **26** 032111
- [26] Fredrickson E., Gorelenkov N.N., Bell R.E., Diallo A., LeBlanc B.P., Lestz J. and Podestà M. 2021 *Nucl. Fusion* **61** 086007
- [27] B.N. Breizman, M.B. Dreval, S.E. Sharapov submitted to *Phys. Plasmas* (2025).
- [28] S. E. Sharapov et al 2014 *Physics of Plasmas* **21** 082501
- [29] I.H. Hutchinson, Principles of Plasma Diagnostics 2<sup>nd</sup> Edition (Cambridge University Press, 2005).
- [30] M J Hole, L C Appel, R Martin *Rev. Sci. Instrum.* **80**, 123507 (2009)
- [31] M B Dreval et al. *Nucl. Fusion* **65**, 016043 (2025)
- [32] Morris W et al. 2014 *IEEE Trans. Plasma Sci.* **42** 402
- [33] Gee S J et al. 2005 *Fusion Engineering and Design* **74** 403
- [34] M Cecconello et al 2023 *Plasma Phys. Control. Fusion* **65** 035013
- [35] J. W. S. Cook, 2022 *Plasma Phys. Controlled Fusion* **64** 115002
- [36] Slade-Harajda, Cook et al 2025 *Phys. Plasmas* **32** 082506
- [37] P Schild et al 1989 *Nucl. Fusion* **29** 834.
- [38] B C G Reman et al 2022 *Plasma Phys. Control. Fusion* **64** 085008
- [39] V G Kiptily et al 2022 *Plasma Phys. Control. Fusion* **64** 064001